Investigating the Effects of Bubble Distribution on the Heat Transfer in a Nucleate Pool Boiling of Surfactant Solution

K. M. K. Pasha

Associate Professor of Mechanical Power, Faculty of Engineering, Modern University, Cairo, Egypt

Abstract: **- The present work is a continuation of my previous work in which, an experimental investigation was accomplished for the nucleate pool boiling of an aqueous solution of surfactant. The surface temperature and the ambient surfactant temperature are measured for three tubes that are made of brass, aluminum, and stainless steel with almost the same surface roughness. Each one of these tubes is tested with three aqueous solutions of surfactant; TRITON X-100, SLES, and SDS. Each one of the three aqueous surfactant solutions is investigated at concentrations of 0, 200, 500, 1000 and 1500 ppm. This concentration range is different from that used in my previous work to allow additional validation for the studied phenomena. To relate the bubble distribution to the heat flux, the measured superheat temperature and heat flux along with their corresponding surfactant physical properties of the solution are fed into suitable published relations that relate the bubble distribution to the minimum cavity radius. From these relations, it was possible to suggest three formulas that correlate the heat flux to the bubble distribution, the measured superheat temperature and the type and concentration of the used surfactant. The experimental investigations showed that, for all cases, the density of bubble distribution increased with the superheat temperature, the heat flux, and the surfactant concentration. For TRITON-X, the bubble distribution increased with the increased surfactant concentration until the value of about 500 ppm, and beyond this value, the distribution varied very slightly.**

Keywords:- **Heat, Pool Boiling, bubble, Surfactant**

Nomenclature and Abbreviations

Alphabetic

A	**The heated area of the test tube, m^2.**
c	**Concentration, ppm.**
c_l	**Liquid specific heat, kJ/(kg.K).**
D_b	**Bubble diameter, m.**
f	**Bubble frequency, 1/s.**
g	**Gravitational acceleration, m/s^2.**
h	**Heat transfer coefficient of the surfactant solution, $W/(m^2.K)$.**
I	**Current, amp.**
m	**Exponent of the distribution function**
N	**Number of active nucleation sites**
N(r)	**Distribution function for the radii of stable nuclei**
p	**Pressure, N/m^2.**
q	**Heat flux, W/m^2.**
r	**Bubble radius, m.**
rst	**Maximum value of (r); which corresponds to the nucleation starting (N= 1), m.**

Ra, Rq, Rt, Ry and Rz surface roughness parameters defined by DIN 4762 μm.

rc	**Minimum radius of nucleation sites, m.**
T	**Fluid temperature, K.**
V	**Voltage, Volts.**

Greek symbols

θ	**Contact angle, degrees.**
η	**Dynamic viscosity, $N.s/m^2$.**
λ	**Liquid thermal conductivity, $W/(m^2.K)$**
ρ	**Mass density, kg/m^3**
σ	**Surface tension of liquid–vapor interface, N/m.**

Subscripts

b	**Bubble leaving the heated surface.**
c	**Surface cavity.**
fg	**variation during phase change.**
l	**Saturated liquid.**
max	**Maximum number of active nucleation sites.**
nc	**Natural convection.**
nuc	**Nucleation.**
s	**Tube surface condition.**
sat	**Saturation condition.**
v	**Saturated vapor.**
w	**Pure distilled water.**

Abbreviations

DAQ	**Data acquisition.**
PID	**Proportional, Integral, and Differential.**
SDS	**Sodium dodecyl sulfate.**
SLES	**Sodium lauryl ether sulfate.**
TRITON-X 100	**Octyl phenol ethoxylate with 9-10 moles of ethylene oxide.**

I. INTRODUCTION

The heat transfer from a surface to a single-phase liquid depends mainly on the convection mechanism. But, when a phase change occurs during the boiling process, the bubble behavior produces an additional heat transport mechanism. The heat transfer in a boiling process is greatly affected by the bubble behavior (merging, frequency, growth, detaching, departure, coalescence, and age. The bubbles formation and activities constitute a major part of the heat transfer enhancement. The bubble behavior is affected by many factors which include the superheat temperature, the dynamic and equilibrium surface tensions, the liquid properties, the gravity, and any other force fields. The surface position and its roughness play essential roles in the nuclei formation and bubble removal. These are beside the other effects from the physisorption and electro-kinetics actions at the liquid-solid interface and the Marangoni effect [1]. In phase-change processes, the primary mechanisms may be related to the liquid-vapor interfacial tension, and surface wetting at the solid-liquid interface. At the *micro-scale*, and during nucleation and bubble growth, the transient transport mechanisms at the solid-liquid-vapor interface can be attributed to the thin-film spreading and the micro-layer evaporation. But, at the *macro-scale*, the heat transport is governed by the bubble growth and distribution, macro-layer heat transfer, bubble dynamics (bubble translation, coalescence, collapse, and break-up). The adsorption of ionic surfactants, in particular, at the solid-liquid interface alters the behavior of the solid surface considerably. Based on this adsorption process, the electrokinetics and wettability behaviors of the solid surface can be explained by the ions exchange in the electro-kinetic double layer, and are directly reflected in the change in zeta effect. The adsorption of ions and molecules of the surfactant in the interface region plays an important role in the bubble growth and detaching. This phenomenon is controlled mainly by the charge and potential distribution between the different phases, which itself determines the interaction energy between the molecules or particles. The type of relative motion between the different phases determines electrokinetic or zeta potential effects. For the surfactant adsorption at the solid-liquid interface, the streaming zeta potential will arise when the solution is in contact with the stationary surface [2]. The interfacial characteristics can be significantly *altered* and decoupled by introducing small quantities of additives in the water such as surface-active polymers [3]. So, bubbles that contain high vapor content may form at a lower temperature difference. So, the bubble frequencies increase and the lifetime of each bubble decreases. Each bubble flows upwards due to the buoyancy effect and collapse after a certain time to share the heat in the vapor content to surrounding water. Adding surfactant leads to a considerable improvement in the hydrophilic mechanism that affects the bubble dynamics and accordingly, enhances the pool boiling heat transfer. With the nucleation of a vapor bubble and during its subsequent growth, the diffusion of surfactant molecules, and their adsorption rates at the interface govern the extent of dynamic surface tension. The relation between the amount of additive and the reduction in surface tension is not linear, but asymptotic. [4] tested the surface tension for alcohol/water mixtures, and the alcohol mass fraction ranged from 0 to 1 and added Perfluoroalkyl to these mixtures at concentrations ranged from 0 to 5000 ppm. They reported that the surface tension decreased with the concentration until a mass fraction of 0.5 and beyond this value, the reduction rate decreased considerably to approach the value of 10 mN/m. [5] tried to interpret the reduction in surface tension with the concentration of Sodium Dodecyl Sulfate (SDS) which is one of the surfactants used in the present work. They reported that the molecules of the added SDS surfactant disturb the bonding cohesive and adhesive forces between water molecules and with a solid surface. That increases the possibilities of bubble growth and detaching from the heating surface even at the low-temperature difference. Since the surfactants play essential roles in the heat transport process, many researchers investigated the effects of adding different surfactants on the boiling process. Investigating the surfactant SDS (anionic surfactant “sodium dodecyl sulfate") and pure water showed a similar trend of variation in the heat transfer enhancement with surfactant concentration for different heat fluxes. The enhancement could reach a value of 73% for a concentration of 700 ppm and heat flux of 400 kW/m^2. For the same conditions and with the increase in concentration, the surface tension may decrease asymptotically, while the viscosity continues to increase [6]. The boiling process of aqueous solutions of surfactants; (SLS), ECOSURF™ EH-14, TRITON X-100, SDS, and ECOSURF™ SA-9 were investigated. This investigation showed that the reduction in surface tension leads to a higher nucleation site density. And the bubble departure frequency was higher than that of pure water [7, 8, 9]. When testing the SLS aqueous solution, an optimum boiling heat transfer augmentation of about 66.27% was achieved [10]. Investigation of the nucleate pool boiling heat transfer characteristics was performed by [11] for different aqueous surfactant solutions; 99% sodium dodecyl sulfate (SDS) and TRITON X-114. He observed a reduction in surface tension and changes in the bubbles contact angles for a range of heat flux (24.7-109.1 kW/m^2) and mass concentrations (50-8000 ppm for SDS and 20-1000 ppm for TRITON X-114). One of the important regions is the neighboring liquid-vapor interfaces of the thin liquid film contained between bubbles. The force of repulsion resulting from the interaction of surfactants adsorbed at this region is strong enough to overcome buoyancy and surface tension forces [12]. In the present work, the heating surface is a horizontal tube surface. This surface maybe divided into two areas; upper and lower. In the lower half, the buoyancy force has a large component along the same direction of surface tension, and accordingly, the possibility of bubbles removal is reduced considerably. In such a case, adding a surfactant to

the boiling water may improve the characteristics of the interfacial region. Accordingly, the bubble removal from the inverted heater will be easier. It is intended to accomplish the following tasks;

1. Experimental investigation of the superheat temperature and heat flux in the nucleate pool boiling process. The three tested surfactants are; TRITON X-100, SLES, and SDS. Each one is tested at concentrations which are; 0, 200, 500, 1000 and 1500 ppm. Three horizontal tubes are used as boiling surfaces, which are made of Brass alloy C44400, Aluminum alloy 6061 and Stainless steel 316 L. 2).
2. For each investigated case, the measured superheat temperatures and their corresponding heat flux and the surfactant solution properties are fed into suitable published relations.
3. Suggesting correlations for the heat flux, the superheat temperature, the surfactant concentration, and the bubble distribution for each surfactant solution.

II. EXPERIMENTAL PREPARATIONS

2.1 The Test Rig

A controllable test rig is prepared to investigate the heat transfer in a nucleate pool boiling process in which, three horizontal heated tubes are cooled by three different types of aqueous surfactant solutions with different concentration values. Figure 1 shows a schematic diagram of the experimental test rig.A ***more detailed*** diagram of the test rig is illustrated in appendix (C). It consists of the following main components;

2.1.1. Boiling and Condensation Vessel

It consists of two stainless steel (316 L) hollow cylinders of different diameters connected by semi-conical shape 80 mm height. The upper cylinder has dimensions of 264 mm inner diameter, 280 mm outer diameter, and 200 mm length, and it contains a cooling coil, which is used in condensing the vapors of the aqueous solution.

The lower cylinder has inner diameter, outer diameter and length of150 mm, 166 mm and 200 mm, respectively, and it contains the test tube, (2), the auxiliary heater, (3), whose diameter and maximum power are 120 mm and 2kW, respectively, and a motor-driven stirrer, (4). It has two glass windows (90 mm diameter each), which are perpendicular to each other, and whose centrelines are at the level of 100 mm from the bottom. These two glass windows are used for visual observation of bubble formation at the test tube. The vessel is well insulated by a 2 cm-thickness layer of Polyurethane foam (Thermal conductivity is 0.023 W m-1 °C-1). A pressure sensor, (P) is fitted to the top wall of the vessel. The test tube is fixed to the sidewall flange so that; they have the same centerline. The vessel bottom is provided with a drainage port that discharges the required amount of the aqueous solution to the high concentration tank. Another sealed port surrounds the stirrer shaft, which has the same centerline as the auxiliary heater. Two temperature sensors, (T), are fitted to the inlet and outlet of the condensing coil. Another temperature sensor is secured inside the vessel on the gas side, which monitors the saturation temperature. The three temperature sensors are interfaced to the computer through the NI USB 6210.

2.1.2. Test Tubes (Boiling Surface), Figure 1

The test section consists of a horizontal hollow tube (made of either brass, aluminum alloy 6061 or stainless steel 316L), whose outer diameter, inner diameter, and length are 22, 15, and 120 mm, respectively. It contains an electric cartridge heater (100 mm long, 220 V and 1 kW), whose insulated lead wires are press-fitted inside the test tube using conductive grease. This grease fills any remaining air gaps and provides a good heat transfer. The heater is centrally located inside a copper tube and insulated from both ends to minimize the axial heat loss. The outer surface of each one of the three test tubes is treated mechanically by applying successive sandpapers with different roughness degrees; 400, 800, 1000, 1200, 1500, 2300, and4000 grit). After that, the surface is polished with a polishing powder, cleaned with acetone, rinsed with a distilled water and dried by hot dry air.

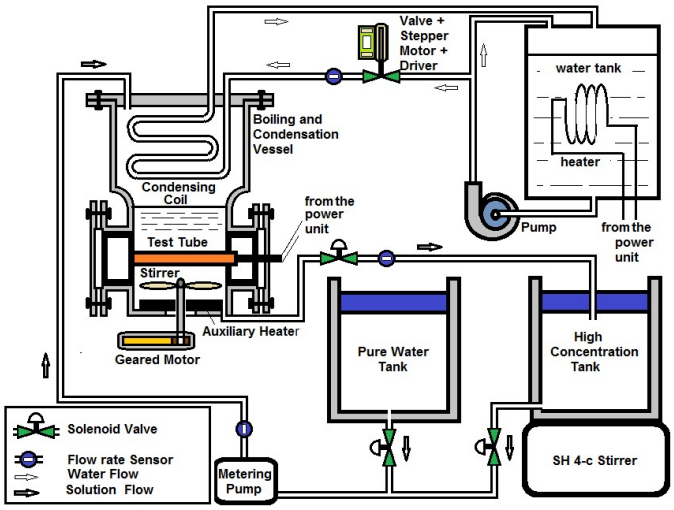

Figure 1 the Experimental Test Rig

The roughness of the three surfaces is then tested using a surface profile-meter, which checks the parameters Ra, Rq, Rt, Ry, and Rz, that are defined by DIN 4762. The tube surface temperature is taken as the average of the readings that are measured by eight copper-constantan thermocouples. These thermocouples are fitted to the tube surfaces by embedding them in longitudinal grooves, that are notched underneath the test tube surface, and are 1 mm depth, and these the thermocouple are distributed uniformly through the surface. Another four copper-constantan thermocouples are distributed around the tube to measure the liquid bulk

temperature. The twelve thermocouples are used in calculating the heat transfer coefficient and are connected to a data acquisition system that receives all their output signals, and converts them into a spreadsheet data by the aid of special software.

2.1.3. Cooling Water Circuit

The cooling water circuit is used to absorb the boiling latent heat of the aqueous solution. This circuit works with the auxiliary heater to maintain the aqueous solution at constant saturation temperature under the saturation pressure. The water leaves the tank, (12) to the circulating pump, (10), which is of type Bosch PA66-GF30, brushless and 17.5 liters/min. It supplies the condenser coil, (14), with the cooling water. The water rate is controlled by a valve, that is driven by a stepper motor with its driver. The water flow rate is first roughly estimated according to the tube heater power, and after starting, the program keeps adjusting it according to a PID technique until achieving steady saturation conditions inside the vessel.

2.1.4 The Tanks

Three tanks are used in this test rig;

- The cooling water tank, (12), whose capacity is 80 liters, and contains two ports on its top; one to receive the return water from the condensing coil, and the other is to receive the water from the bypass line. Another port is located in its bottom through which, the water is delivered to the circulating pump. The water temperature is monitored by a thermocouple that is interfaced to the computer through the acquisition unit. A 2 kW heater, (11), is switched ON when the temperature decreases below the required temperature.

2.1.5 Measuring and Control Devices

The following paragraph is a brief description of the used measuring and control devices, that are used in the test rig;

-The controller is an 8051 Architecture Microcontrollers; a rich Atmel portfolio of MCUs based on the 8051 instruction set.

-The acquisition system type is an NI USB- 6210, input, 16-bit resolution and 256 ks/s

-The metering pump is WEA, HY Series with a diaphragm PTFE. Its frequency is from 0 to 160 Strokes/minute. It works at 230-volt VAC 50/60 Hz and discharges from 0 to 3.0 Liters/min

-Flow Rate Sensors; Model Fs 300 AG, 3/4″ Fitting, Flow rate: 1~60 L/min, max, Working Current: 15mA (DC 5V).

-Temperature sensor; The TMP36, 10 mV/8°C Scale Factor, ±1.5°C Accuracy, Less than 50 µa Quiescent Current, and is located in the water tank, the vessel and the condenser coil.

- copper-constantan thermocouples with ± 0.5 accuracies and are interfaced to an acquisition system.

- A valve that is controlled by DC servo motor rotates according to a National Instrument's (NI) DAQ Board, Lab view real-time software, and the PCI extensions for instrumentation (PXI)

-Pressure Transducer Sensor; SKU237545, and is located at the top of the condensation vessel

-Magnetic Stirrer; Faithfulsh-4c Ceramic, Model NO.: SH-4C, Certification: CE, ISO, Max Vol.: 5000ml, 220V/ 110V

- the physical properties of *samples* of surfactant solution at the temperatures and ***concentrations*** used in the experiments were estimated using the following devices; du-nouy ring tensiometer to measure the surface tension, pycnometer to measure the density, rheometer for the viscosity

2.2. Experimental Procedure

Prior to performing the experiments, the test sections are cleaned routinely before and after each test run with a sequence of operations involving washing with alcohol, rinsed with distilled water several times and dried by a supply of hot dry air. Then, the system is evacuated to a pressure of about 15 mm Hg. If no leakage is detected over a 24 hours interval, then the test rig is ready for the *Experimental procedure*, which is detailed in appendix 'C'.

-The high concentration tank, (6), whose capacity is five liters, and it contains a surfactant aqueous solution of concentration 3000 ppm This tank is used to supply the vessel with a high concentration aqueous solution to produce the required mixture concentration in the vessel. The solution, which is returned from the vessel enters the tank through a port in the top cover. The tank bottom includes a port through which, the aqueous solution can move to the metering pump. The tank is supported by a magnetic stirrer in order to ensure a uniform concentration.

-The distilled water tank, whose capacity is five liters too, and it contains a pure distilled water. This tank is used to supply the vessel with a distilled water to produce the required mixture concentration in the vessel. The required amount of distilled water leaves the tank to the metering pump through a port in the tank bottom. The cover on the top of anyone of the last two tanks is capable of sliding vertically up and down to allow the inner space to expand or contract when it receives or supplies any amount of the aqueous solution. Also, the cover weight on the top of the liquid slightly increases the pressure inside the tank, and that aids the discharging process from the tank to the metering pump, (5).

2.3 Data Acquisition

$h = q_s''/ \Delta T$ (1)

Where q" is the heat flux=I V/A_s and ΔT is the superheat temperature = (Ts - Tsat).

Calculation of nucleate site density, N/A

$Q = Q_{nc} + Q_{nuc}$ (2)

or, $q.A = q_{nc}.A_{nc} + q_{nuc}. A_{nuc}$, and consequently,

$h - h_{nc} = (h_{nuc} - h_{nc}). (A_{nuc} / A)$ (3)

and the effective area for a single active site is, $\pi.D_b^2$

D_b, the diameter of the bubble when leaving the heated surface, then, for N active sites,

$A_{nuc} = N. \pi D_b^2$ (4)

According to [13];

$$\frac{N}{A}.\pi.D_b^2 = \frac{(h - h_{nc})}{(h_{nuc} - h_{nc})} \quad (5)$$

N/A number of active nucleation sites per surface area

D_b, the diameter of the departed bubble which could be estimated using Fritz model [14] along with the estimated surfactant properties from [7];

$D_b = 0.0208\ \theta.(\sigma/g\ (\rho_l - \rho_v))^{0.5}$ (6)

The convective heat transfer coefficient According to [15];

$h_{nc} = 0.15\ [\ (g^*\ \beta^*\ c_l\ (\rho^*\ \lambda_\lambda)^2\ )/\eta]^{1/3}\ \Delta T^{*1/3}$ (7)

nucleate heat transfer;

$h_{nuc} = 1.1284\ [\ (\rho_l\ c_l\ \lambda_l\ )^{0.5*}\ f^{0.5}$ (8)

$$f = [\frac{0.314 g(\rho_l - \rho_v)}{D_b \rho_l}]^{0.5} \quad (9)$$

the minimum cavity radius, r_c, from [7, 13];

$$r_c = [\frac{2.T_{sat}^* \rho_l}{h_{fg} \Delta T}] \quad (10)$$

So, we may use the experimental data of the investigated cases of different heat fluxes, surfactant concentration, and heat fluxes, along with the surfactant solution properties [2] in order to calculate N/A and r_c for different ΔT and accordingly, to relate N/A to r_c as follows;

$$\ln(\frac{N}{A}) = \ln\frac{N_{\max}}{A}.(1 - (\frac{r_c}{r_{st}})^m) \quad (11)$$

where Nmax is the maximum value of N (at $r_c = 0$), r_{st} is the maximum value of r_c which corresponds to the nucleation beginning (N = 1), and m is an exponent. The values of N max, r_{st}, and m are experimentally determined and they depend mainly on the boiling fluid concentration. Correlations are made to correlate the size distribution function's constant (m, r st St and N max/A) using obtained heat transfer measurements for different aqueous solution concentration.

2.4 Data Validation

The results of the present experimental work, for the heat flux and the superheat temperature, were compared to those of the previous work of both Elghanam [7] and Wen [16]. Figure 2 illustrates a comparison of the present data of the heat flux

and the superheat temperature, for the case of TRITON surfactant with concentration 500 ppm on an Aluminum tube with those of the previous work of both; Wen and Elghanam. Figure 3 illustrates another comparison of the present data with Elghanam and Wen at the same conditions, but for the surfactant SDS. It is obvious that the curves of the present work have the same trends as those of Elghanam and Wen, but the data are slightly higher than those of Elghanam and lower than those of Wen. This may be because,

Elkhanam used one thermocouple to measure the solution temperature, which does not ensure a uniform saturation temperature everywhere in the solution, especially, with the heat losses, which vary from position to another in the vessel. In such conditions, the acquisition system may receive temperature readings that indicate higher temperature differences than those of the present work for the *same apparent* heat flux and, or in other words, lower heat flux for the same temperature difference. In the present work, four thermocouples are used to measure the solution temperature in different positions of the solution. That is besides a temperature sensor, which continuously allows the controller to adjust the cooling flow rate, the tube heater, auxiliary heater, and the stirrer in order to ensure that, no position in the liquid has a temperature *lower* than the saturation value. Lower temperature leads to a higher temperature *difference*. Wen used a horizontal plate, which reduces the chances of bubble coalescence, and accordingly, reduces the possibility of forming larger bubbles that move upward at a lower velocity and imparts the heat transfer process.

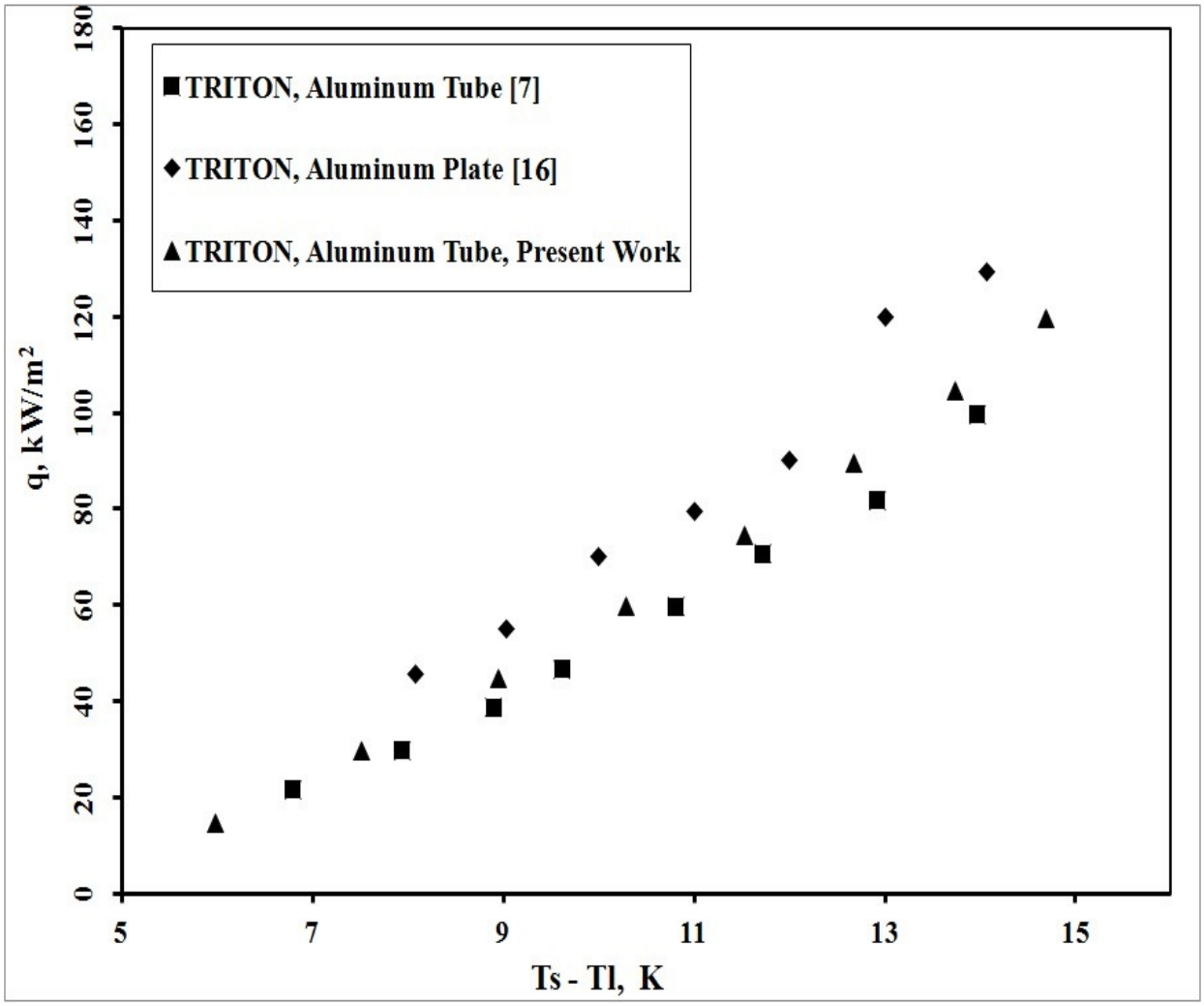

Figure 2 Comparison Of Data For TRITON Surfactant At Concentration Of 500 Ppm With the work of Elghanam(2011) and Wen(2002).

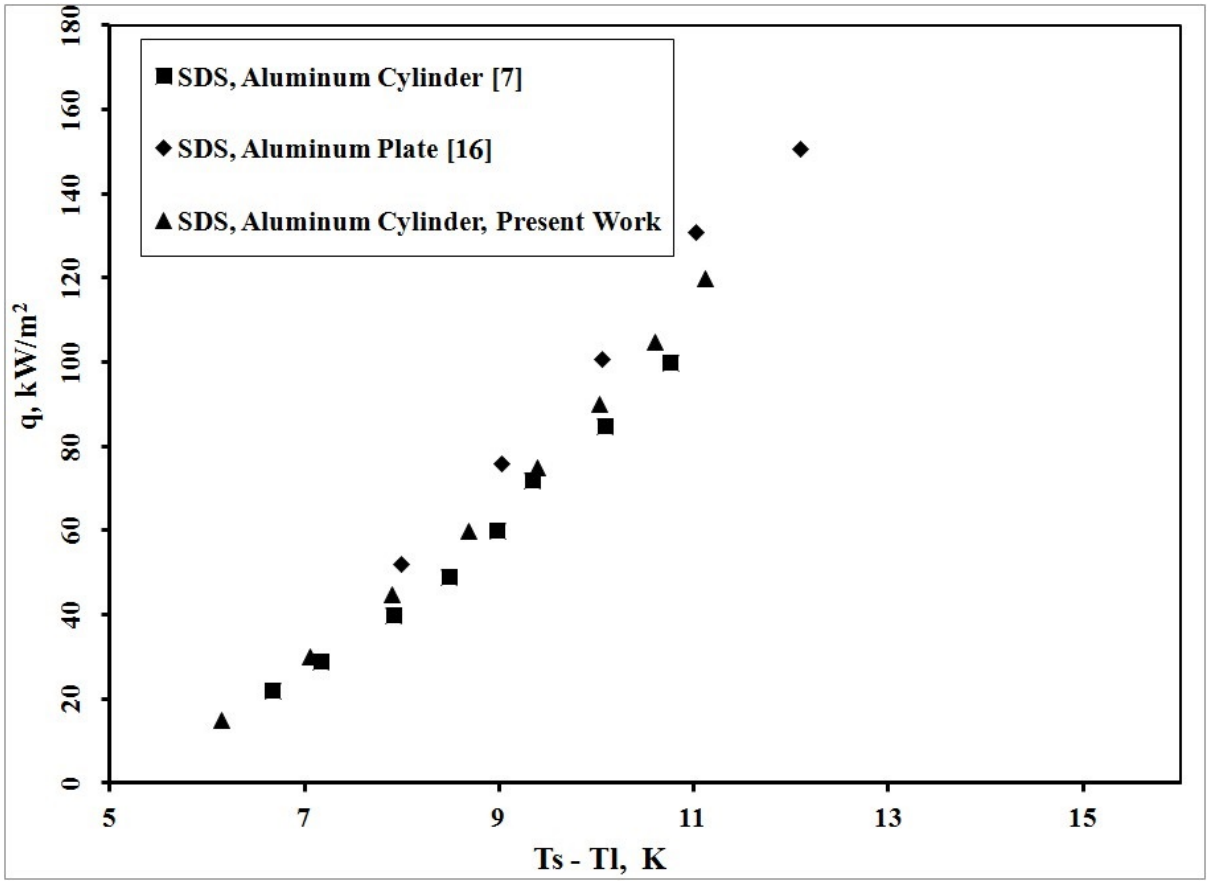

Figure 3 Comparison Of Data For SDS Surfactant At Concentration Of 500 Ppm with the work of Elghanam(2011) and Wen(2002).

III. RESULTS AND DISCUSSION

As mentioned earlier, the bubble formation and dynamics were proved to have a considerable role in the heat transfer process. In the present work, the experimental work aimed to investigate the relations between the heat flux and superheat temperature and the bubble formation in the pool boiling processes of aqueous solutions of three surfactant types. Figure 4 illustrates the variations of the bubble density with both; the heat flux and the superheat temperature for the three surfactants, TRITON, SLES, and SDS. The figure indicates that, for all cases, both the heat flux and the superheat increased with the bubble density. The increased heat transfer may be caused by the agitation effect resulted from the mobility of the vapor bubbles leaving the tube surface, and this mobility promotes for more turbulent activity and better mixing and transport process. The increase in the superheat temperature promotes for a greater number of nucleation sites. For the same heat flux and superheat temperature, the bubble density increased with the surfactant concentration for all cases of SLES and SDS. That may be because increasing the concentration of aqueous surfactant solution affects the dynamic surface tension, and modifies bubble dynamics. With the nucleation of a vapor bubble and during its subsequent growth, the diffusion of surfactant molecules, and their adsorption rates at the interface govern the extent of dynamic surface tension. The dynamic surface tension is lower than solvent's surface tension, and that helps promote a large number of active nucleation sites and allows the departure of smaller-sized bubbles because of the reduction in surface tension force at the heated tube wall that counters the buoyancy force. The bubble growth time is consequently reduced, and that leads to an increase in bubble departure possibilities. But, in case of TRITON-X, the bubble density increased considerably until the concentration of 500 ppm, and beyond this value, it slightly increased. This may be related to the fact that the variation of surface tension with concentration for TRITON X-100 is constant above solution concentration of 500 ppm, and accordingly, the promotion of the bubble formation varies slightly beyond the concentration of 500 ppm. Also, increasing the concentration of this high molecular weight substance decreases the convective heat transfer, which helps the phase change and promotes for more bubble formation. It is observed that, in all cases of TRITON and SLES, and with the *increase* of heat flux and superheat temperature the *rate of increase* in the bubble density starts to decrease. The reason may be that, for any surfactant, the bubble formation increases with the heat flux, and its increased mobility helps the thermal transport, but, the gaseous phase inside the bubbles has a lower thermal

conductivity. And that may be an opposing factor, which leads to a decrease in the heat transfer activity and decreases the ability to form more bubbles. In case of SDS surfactant, and for concentrations, that exceeds 500 ppm, the *rate of increase* in bubble density starts to increase with the superheat temperature. This reflects the effect of increasing the convective heat transfer for the low molecular weight substance, which dominates after achieving the surfactant concentration of 500 ppm and helps the formation of more bubbles. From the experimental data, we can get the bubble distribution and the critical bubble radius as functions of the superheat temperature, equations 9 and 10, and accordingly, we can get the size distribution function, equation 11. Figure 5 illustrates the effects of surfactant concentration on the size distribution function's constants (m, Nmax /A, and r_{st}), that could be obtained from the experimental data. It is observed that, for TRITON, N_{max}, increased until the concentration of 500 ppm, and beyond this value, it varied very slightly, but for both SLES and SDS, it kept increasing with the surfactant concentration. The bubble density increases with this constant, so, this agrees with the bubble density variation illustrated in figure 4. Also in the case of pure water, the bubble density increased with the superheat temperature at a smaller rate compared to those of the surfactant solutions, and that reflect the considerable effect of the curfactant on the solution surface tension which in turn, helps increase the rate of bubble formation.

Most of the previous researchers correlated the heat flux to the *bubble distribution* and the *superheat temperature* through constants, that are functions of concentration, [12]. In the present work, when relating the bubble distribution and the minimum radius of nucleation to the measured data, it is possible to suggest the following correlations, that relate the effects of bubble distribution, superheat temperature and surfactant concentration to the heat flux;

$$q = a\,(T_s - T_l)^b\,(N/A)^c\,(C)^d \qquad \text{kW.m}^{-2}, \quad (12)$$

for TRITON, a = -0.95 , b = 1.26 c = 0.29 d = -0.02

for CLES, a = -0.72 b = 1.14 c = 0.37 d = -0.06

for CDS, a = -1.18 b = 1.1 c = 0.49 d = -0.03

Appendix (A) illustrates comparisons of the experimental data and those calculated from the correlations, equation (12). The worst percentages of deviation of the calculated data using these correlations is less than 5%

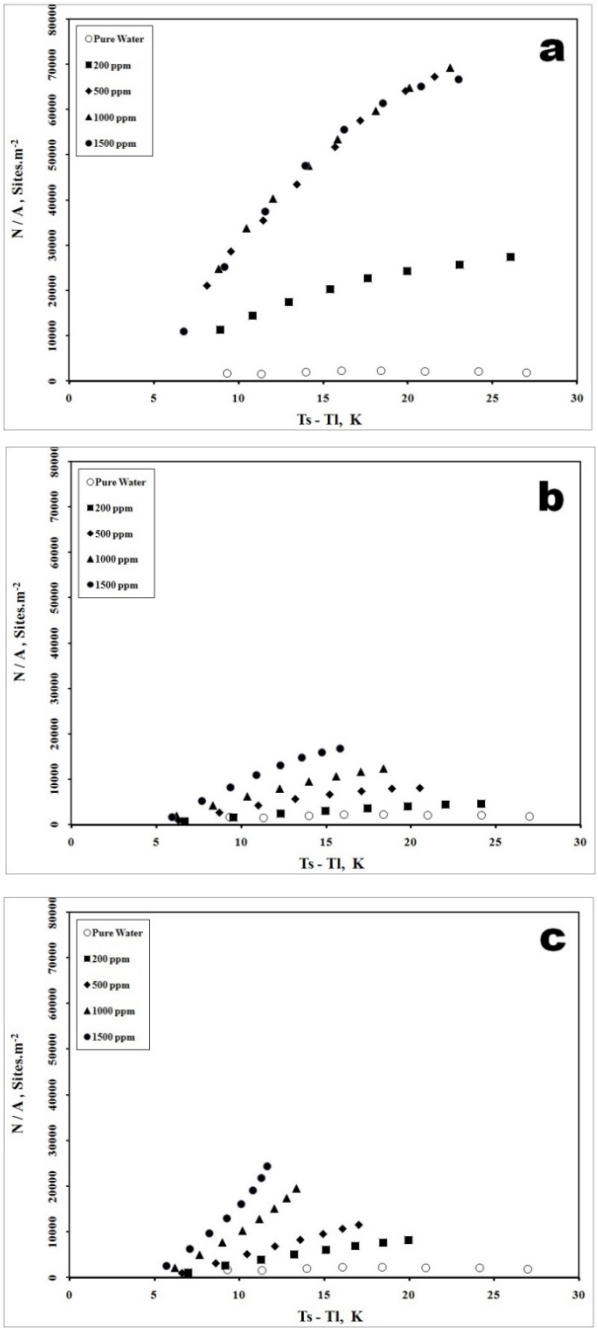

Figure 4 Variations Of The Bubble Density With The Heat Flux And The Superheat Temperature.

a) Variations Of The Bubble Density With The Superheat Temperature For TRITON.

b) Variations Of The Bubble Density With The Superheat Temperature For SLES.

c) Variations Of The Bubble Density With The Superheat Temperature For SDS.

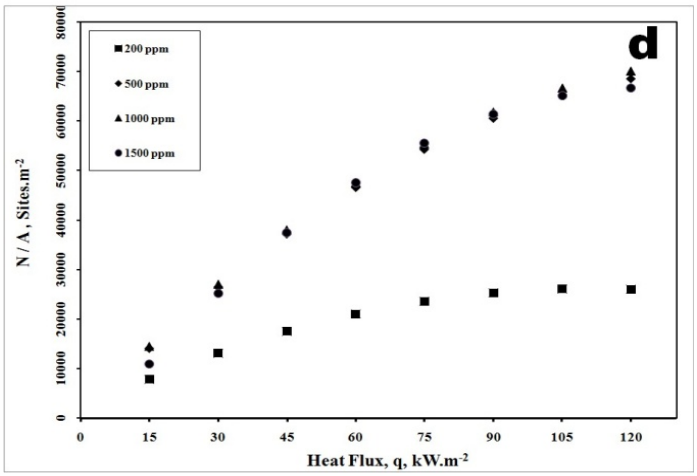

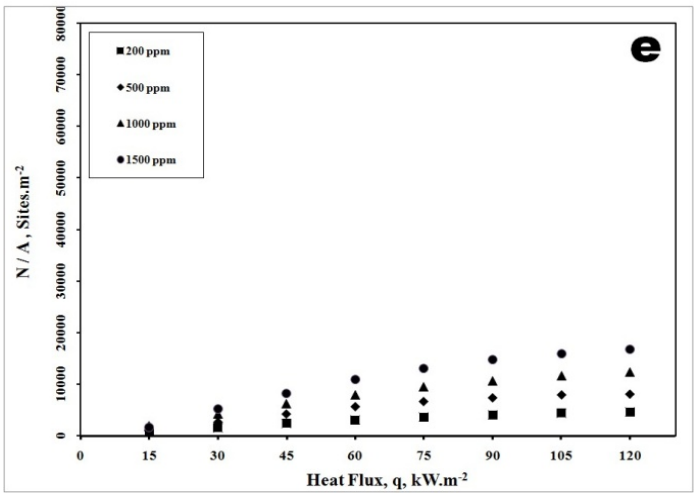

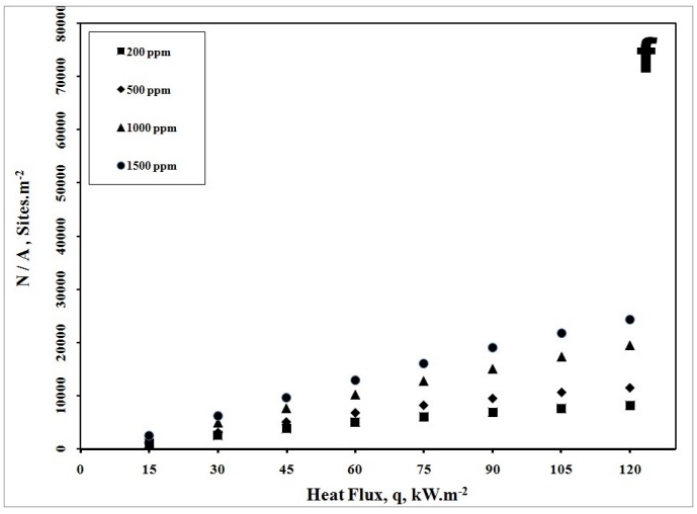

Figure 4, Cont.

d) Variations Of The Bubble Density With The Heat Flux For TRITON.

e) Variations Of The Bubble Density With The Heat Flux For SLES.

f) Variations Of The Bubble Density With The Heat Flux For SDS.

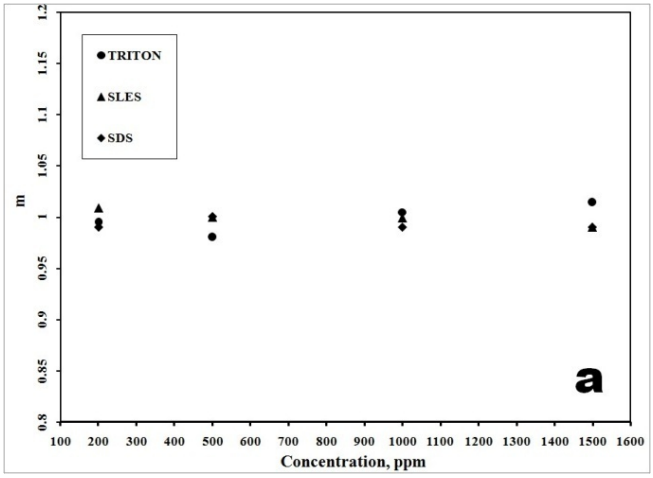

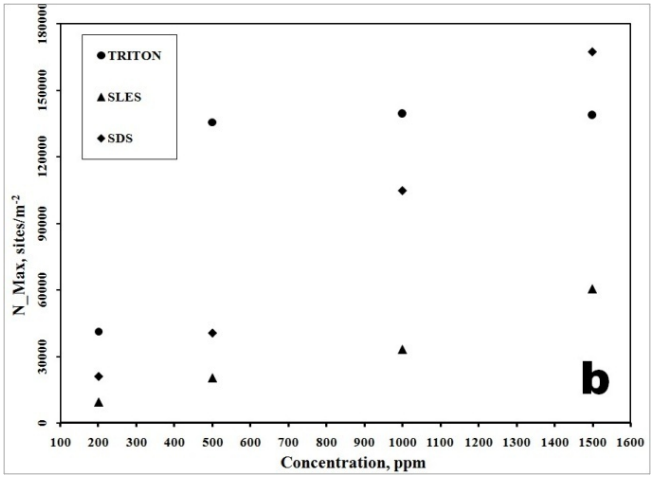

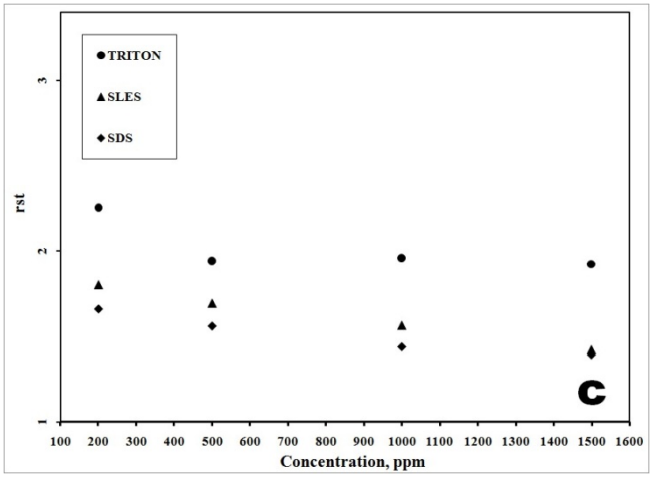

Figure 5 Variations Of The Distribution Function Constants, m, $N_{max,}$ and r_{st}, With The Surfactant Concentration.

a) Variations Of The Distribution Function Constant, M With The Surfactant Concentration.

b) Variations Of The Distribution Function Constant, N_{max} With The Surfactant Concentration.

c) Variations Of The Distribution Function Constant, r_{st} With The Surfactant Concentration.

IV. CONCLUSION

The present work is an experimental investigation of the heat flux and the superheat temperature in a pool boiling process. *Three* tubes are made of brass, aluminum, and stainless steel with almost the same surface roughness. Each one of these tubes is tested with *three* aqueous solutions of surfactant; the anionic Sodium Dodecyl Sulfate,

(SDS), the anionic Sodium Lauryl Ether Sulfate, (SLES)and the nonionic Octylphenol Ethoxylate with 9-10 moles of Ethylene Oxide, (TRITON X-100). Each one of the three aqueous solutions is investigated at concentrations of 0, 200, 500, 1000 and 1500 ppm. The experimental data are supplied to formulas, that relates the bubble distribution function to the measured heat flux

and the superheat temperature, and relates the surfactant concentration to the three constants, (m, Nmax /A, and r_{st}) of the size distribution function. The results showed that, when increasing the surfactants concentration, “m” slightly increased, “Nmax/A” considerably increased, and “r_{st}” asymptotically decreased. For the same surfactant concentration, the surfactant TRITON exhibited the highest values of the size distribution function’s constants. For all investigated cases, the bubble density increased with both the heat flux and superheat temperature. *Three* correlations are suggested to correlate the heat flux to the superheat temperature, the bubble distribution and the surfactant concentration for each type of the *three* surfactants. Most of the experimental data fitted well to these correlations, and few values deviated from those, that are calculated from the correlations. The worst percentage of deviation was about 5%.

REFERENCES

[1]. G. Hetsroni, A. Mosyak, and Elena Pogrebnyak, Effect of Marangoni flow on subcooled pool boiling on micro-scale and macro-scale heaters in water and surfactant solutions", International Journal of Heat and Mass Transfer, Volume 89, Pages 425-432, 2015.

[2]. Juntao Zhang, Experimental and Computational Study of Nucleate Pool Boiling Heat Transfer in Aqueous Surfactant and Polymer Solutions, Ph.D. thesis, Department of Mechanical, Industrial and Nuclear Engineering, University of Cincinnati, 2004.

[3]. R. M. Manglik, A. Athavale, D. S. Kalaikadal, A. Deodhar, and U. Verma, Reactor Engineering: Multi-Scale Control and Enhancement of Reactor Boiling Heat Flux By Reagents and Nanoparticles, Technical Report Tftpl-21-Doe-Neer, August 2011, U.S. Department of Energy, University of Cincinnati, Cincinnati, Ohio 45221-0072, 2011.

[4]. Toshiaki Inoue, Yoshio Teruya, Masaru Ishii, and Masanori Monde, Enhancement of Pool Boiling Heat Transfer in Water and Ethanol/Water Mixtures (Effect of Surface-Active Agent), Heat Transfer—Asian Research, 33 (4), PP 229-244 2004.

[5]. G. Suryanarayana, G. Venkateswara Rao, N. And N.Balakrishna, Experimental investigation on Pool Boiling Heat Transfer with sodium dodecyl Sulfate, International Journal of Mechanical Engineering and Computer Applications, Vol3, Issue2, ISSN 2320-6349, pp32-37, 2015.

[6]. G. Hetsroni J.L. Zakin, Z. Lin, A. Mosyak, E.A. Pancallo, and R. Rozenblit, The effect of surfactants on bubble growth, wall thermal patterns and heat transfer in pool boiling, International Journal of Heat and Mass Transfer, 44 485±497, 2001.

[7]. R. I. Elghanam, et al, 2011, "Experimental study of nucleate boiling heat transfer enhancement by using surfactant", Ain Shams Engineering Journal, November 2011.

[8]. Hao Peng, et al, 2011, "Effect of surfactant additives on nucleate pool boiling heat transfer of refrigerant-based nanofluid", Experimental Thermal and Fluid Science (EXP THERM FLUID SCI) 35(6):960-970 · September 2011

[9]. Guodong Xia, Huanming Jiang, RanLiu, and Yuling Zhai, 2014, Effects of surfactant on the stability and thermal conductivity of Al_2O_3/de-ionized water nanofluids, International Journal of Thermal Sciences, Volume 84, October 2014, Pages 118-124

[10]. Basim Qasim and Ali Al-Sukhani, 2014, "Enhancement Techniques for Boiling Heat Transfer", Ms.C Thesis, the College of Engineering, Department of Mechanical Engineering, Embry-Riddle Aeronautical University, Daytona Beach, Florida, November 2014.

[11]. Hu Zicheng, 2011, Pool Boiling Heat Transfer of Aqueous Surfactant Solutions, 28-29 March 2011**, Added to IEEE Xplore:** 15 April 2011.

[12]. M. D. Qaisar Raza, Nirbhay Kumar & Rishi Raj, Surfactants for Bubble Removal against Buoyancy, Scientific RepoRts | 6:19113 | DOI: 10.1038/srep19113, PP 1-9, 2016.

[13]. Griffith P. And Wallis J. D., "The Role of Surface Conditions in Nucleate Boiling", Chemical Engineering Progress Symposium Series, Vol. 56, No. 30, Pp 49- 63, 1960.

[14]. Fritz, W., Berechnung des Maximal volumens von Dampfblasen. Phys. Z. 36, 379384, 1935.

[15]. Y. Han C, Griffith P. 1965 "The Mechanism of Heat Transfer in Nucleate Pool Boiling". Int J Heat Mass Trans 1965;8:887–914.

[16]. Wen DS and Wang BX. 2002, "Effects of Surface Wettability on Nucleate Pool Boiling Heat Transfer for Surfactant Solutions". Int J Heat Mass Trans; 45:1739–47, 2002.

Appendices

Appendix A, correlated data

TRITON X-100		
COEFFICIENTS OF EQUATION,() -0.95 1.26 0.29 -0.023		
q, Experimental	q, Correlation	Percentage%
200 ppm		
15	14.7735	-1.50977
30	28.51	4.32530
45	42.99	-4.44650
60	58.5322	-2.44627
75	74.9849	-0.02011
90	91.5226	1.69173
105	107.684	2.55659
120	122.995	2.49544
500 pp		
15	15.702	4.611031
30	30.2333	0.777502
45	44.9904	-0.02124
60	60.395	0.658317
75	75.985	1.31327
90	91.3696	1.52180
105	106.208	1.15003
120	120.195	0.162864
1000 PP		
15	15.56	3.716730
30	29.4175	-1.94157
45	44.067	-2.07329
60	59.546	-0.75660
75	75.4163	0.555133
90	91.3024	1.44707
105	106.874	1.78492
120	121.832	1.527

1500 ppm		
15	15.2396	1.59707
30	28.5849	-4.71702
45	42.88	-4.71104
60	58.0173	-3.30445
75	73.6742	-1.7678
90	89.5139	-0.54012
105	105.196	0.186825
120	120.363	0.302645
SLES		
COEFFICIENTS OF EQUATION -0.72 1.14 0.37 -0.059		
q, Experimental	q, Correlation	Percentage%
200 ppm		
15	14.2611	-4.92600
30	28.5357	-4.88098
45	44.2161	-1.74208
60	60.4422	0.736934
75	76.697	2.26272
90	92.5343	2.81591
105	107.565	2.44302
120	121.439	1.1995
500 ppm		
15	14.24	-5.06611
30	29.7118	-0.96063
45	45.8296	1.84353
60	61.963	3.27171
75	77.6453	3.527
90	92.4163	2.68477
105	105.852	0.811838
120	117.556	-2.03651
1000 ppm		
15	15.812	5.41330
30	31.7859	5.95296

45	47.0284	4.50745
60	62.3533	3.92218
75	77.3257	3.10091
90	91.567	1.74112
105	104.758	-0.23094
120	116.622	-2.81523
1500 ppm		
15	15.1114	0.742674
30	30.6807	2.26908
45	45.3904	0.867605
60	59.7012	-0.49800
75	73.3487	-2.20168
90	86.0235	-4.41829
105	100.439	-4.34380
120	114.086	-4.92751
SDS		
COEFFICIENTS OF EQUATION -1.18125 1.10433 0.486123 -0.031406		
q, Experimental	q, Correlation	Percentage%
200 ppm		
15	14.246	-5.02664
30	29.3323	-2.22562
45	45.0442	0.09817
60	61.1752	1.95869
75	77.2988	3.06513
90	93.0152	3.35025
105	107.968	2.82714
120	121.845	1.53728
500 ppm		
15	14.1934	-5.37721
30	29.2441	-2.51954
45	45.7556	1.67909
60	62.0737	3.45624
75	77.7489	3.66514

90	92.3344	2.59379
105	105.447	0.42577
120	116.769	-2.69252
1000 ppm		
15	15.7962	5.30811
30	31.4217	4.73893
45	46.4554	3.23426
60	61.349	2.24832
75	75.7797	1.03961
90	89.4148	-0.65020
105	101.956	-2.89914
120	113.143	-5.71391
1500 ppm		
15	15.7690	5.12666
30	31.7553	5.85089
45	46.6995	3.77663
60	61.1764	1.96071
75	74.7974	-0.27011
90	87.1816	-3.13158
105	99.1959	-5.52771
120	114.195	-4.83751

Appendix B,

Error analysis

In the present work, the basic measured values are the superheat temperature and the heat transfer coefficient, and so the estimated errors may are as follows;

To estimate the uncertainties of the derived quantities, δA, δT and δh, we first recall the uncertainties of the participating quantities, which are;

The Length: is measured using a vernier caliper with uncertainty 0.02 mm

The temperature, that is used in calculating the heat transfer coefficient, is measured by copper-constantan thermocouples. This type has an accuracy of $\pm$ 0.5 ^{o}C

Then, we can estimate the uncertainties in the derived quantities as follows;

$$\delta A = (\pi d l)\sqrt{(\frac{\delta d}{d})^2 + (\frac{\delta l}{l})^2} \quad \text{B.1}$$

$$\delta Q = (98.3/100)\ x\ V\ x\ I\ \sqrt{(\frac{\delta V}{V})^2 + (\frac{\delta I}{I})^2} \quad \text{B.2}$$

$$\delta h = \frac{Q}{A(T_{s,av} - T_l)}\sqrt{(\frac{\delta Q}{Q})^2 + (\frac{\delta A}{A})^2 + \frac{\delta T_{s,av}^{\ 2} + \delta T_l^{\ 2}}{(T_{s,av} - T_{r,av})^2}} \quad \text{B.3}$$

Substituting the uncertainties in the participating quantities into equation B.3, we can estimate, the worst relative errors in the heat transfer coefficient, δh, which is 4.28 %. This percentage was considered in correcting the calculations

Appendix C

Detailed experimental work

The detailed experimental procedure is described as follows;

1) To prepare five liters of the high concentration solution of the surfactant, (3000 ppm); the SDS surfactant is available as a powder, so, using a precision electronic weighing device, we get 15.05 gm, and adding them to five liters of distilled water. This high concentration solution tank will stay on the stirrer until the end of the experiment.
2) The other two surfactants; SLES and TRITON X-100 are available in liquid form, so, to get five liters of a solution with concentration 3000 ppm, we have to consider the surfactant density. We need, then, to measure 15.00312 ml, which is beyond the pipetting accuracy, so, approximating the amount to 15.003 ml will not considerably affect the concentration accuracy. Adding this amount to five liters of distilled water to get a high concentration solution, (approximately 3000 ppm)
3) To remove the dissolved non-condensable gases, the high concentration solution is delivered to a *separate* container, which includes a variable power electric heater, digital thermometer, and an adjustable check pressure valve. The heater is operated at a power of about 1375 W to heat the solution under atmospheric pressure. After boiling the solution, the heater is kept working for one hour, and During this process, the check valve maintains the pressure at atmospheric value. The heater power is then reduced gradually until the temperature is near the saturation value and then, is maintained for about 45 minutes, Elghanam (2011). Now, the test rig is ready to start the experiment.
4) After installing the test tube, the vessel is charged with three liters of the distilled water to a level of about 120 mm above the top of the test tube surface, Elghanam (2011).
5) The controller *starts the experiment* by increasing the power supplied to the auxiliary heater from zero to its maximum by the gradual increase of the MPW signal, which is sent to the power unit. After achieving the maximum power, the heater keeps working until the temperature sensor indicates the saturation value. The controller is programmed to allow ten seconds delay between any two successive readings for either the pressure or the temperature sensors inside the vessel in order to ensure a correct sense of the trend of change in these quantities.

6) During the heating of the water, the controller keeps reading the pressure and temperature sensors inside the vessel. If the pressure exceeds the atmospheric value, and the temperature is still below the saturation value, that corresponds to the atmospheric pressure, the controller sends a digital signal to the power unit to open the solenoid valve in the vessel until retrieving the atmospheric value. If the temperature inside the vessel started to exceed the saturation, that corresponds to the atmospheric pressure, the controller does not allow the solenoid valve to open, even if the pressure exceeded the atmospheric pressure value because this increase is caused by the increase of temperature above the saturation value. In such a case, the program switches the auxiliary heater off and signals the power unit to operate the circulating pump until retrieving the saturation temperature again.
7) Although the vessel is well isolated but still looses heat to the low-temperature surrounding, these unpredicted losses constitute a steady disturbance to the temperature. So, the controller always uses the decrease in vessel temperature below the saturation temperature as a feedback to a PID technique, that determines the correction in MPW of the signals. These signals are sent to the power unit which determines the required power supplied to the water valve and the auxiliary heater, which will maintain a saturation temperature value inside the vessel.
8) The *steady* values for both the atmospheric pressure and its corresponding temperature are recognized, when the percentage of the difference between any two successive readings of at least five successive readings lies within the range of ∓ 1% of the preceding value. After achieving the steady-state conditions, the controller then, sends two analog signals to the power unit, the first is to supply the test tube heater with about124.3 Watts, which corresponds to a heat flux of 15 $kW.m^{-2}$, and the second is to supply the circulating pump with a power, that corresponds to a discharge, D, where;

   $D = V^2 / R. [\rho\ c\ (T_{in} - T_o)]_w$ (C.1)

   V is the voltage that is applied to the tube heater to produces the required heat flux and R is the heater resistance. T_{in} and T_o are the inlet and outlet cooling water temperatures, that are measured by the two temperature sensors as shown in figure 1. The cooling water is supplied to the vessel to absorb the tube heater energy to help maintain a steady-state. The pressure adjustment procedure, that is mentioned in step (4) is still operated until achieving almost a steady-state pressure and the temperature inside the vessel, with tolerance within the value of ∓ 1%.
9) The program compares the temperature reading of each one of the twelve thermocouples with its previous one. It does not record any temperature reading unless it achieves its *steady-state* condition, which is recognized by the same criteria, which is mentioned in step (7). And it calculates the heat transfer coefficient according to;

   $q_s'' = V^2 / (R.A_s)$ (C.2)

   $h_L = q_s'' / (T_s - T_L)$ (C.3)

   $T_s = \sum_{i=1}^{i=8} T_i / 8$ (C.4)

   $T_L = \sum_{i=1}^{i=4} T_i / 4$ (C.5)
10) When the temperature sensors inside the vessel and in the inlet and outlet ports of the cooling water circuit indicates steady readings according to the criteria, that is mentioned in step (7), the controller then makes 10 minutes delay to ensure that, the acquisition system has recorded the steady readings. Then, the controller starts a new run with a new predetermined heat flux, which exceeds the previous value by 124.3 Watts. And the steps from 4 to 9 is repeated, and so on until, achieving a heat flux of 120 $kW.m^{-2}$, then, the first experiment group is accomplished.

11) The current values of the *surfactant concentrations* in both the vessel and the high concentration tank, figure 1, are zero and 3000 ppm, respectively. To start a new group with a new surfactant concentration in the *vessel*, the *new* surfactant concentration in the *high concentration tank* must be calculated and updated by the controller, as follows;

- The controller opens the pressure port in the vessel *top cover* to compensate for any change in pressure during the change process
- And opens the port in the vessel *bottom* to discharge the vessel solution for a *period of time, t1*. This time is required by the vessel to discharge an amount of solution*, m,* to the high concentration tank. This *time period* is estimated as follow ;

$t_1 = m / D_{vh1}$ (C.6)

$$m = \frac{15\,(C_{v,old} - C_{v,new})}{[\,3\,(C_{v,new} - C_{v,old}) + 5\,(C_{v,old} - C_{h,old})\,]} \quad \text{(C.7)}$$

$C_{v,old}$ the old value of liquid concentration inside the vessel (before each mixing process), (initially, equals 200 ppm)

$C_{v,new}$ the new value of liquid concentration inside the vessel, (after each mixing process)

$C_{h,old}$ the old value of liquid concentration inside the high concentration tank,

(before each mixing process), (initially, equals 3000 ppm)

D_{vh1} discharge from the vessel to the high concentration tank, and, it is determined by the controller and monitored through a mass flow rate sensor, appendix (C).

- The controller switches the vessel valve off and opens the high concentration tank valve on. It then operates the *metering pump* to return the same solution amount*, m,* to the vessel. The metering pump works for a time period, t_2, where;

$t_2 = m / D_{vh2}$ (C.8)

D_{vh2} is the discharge from the high concentration tank to the vessel

and, it is supplied to the controller from another mass flow rate sensor, figure 1. During this process, the motor stirrer is operated and keeps working after the mixing process for five minutes, until the controller switches it off.

12) The changeover from one aqueous surfactant solution to the other must be preceded by a reliable cleaning protocol for ensuring that there are no remaining remnants of the earlier sample inside the boiling condensation vessel. This is achieved by three-cycle operation of cleaning/rinsing with distilled water, acetone, and ethanol, and vacuum drying.

13) The steps from 4 to 12 are repeated until accomplishing the experiments for the three surfactant types besides those of the distilled water

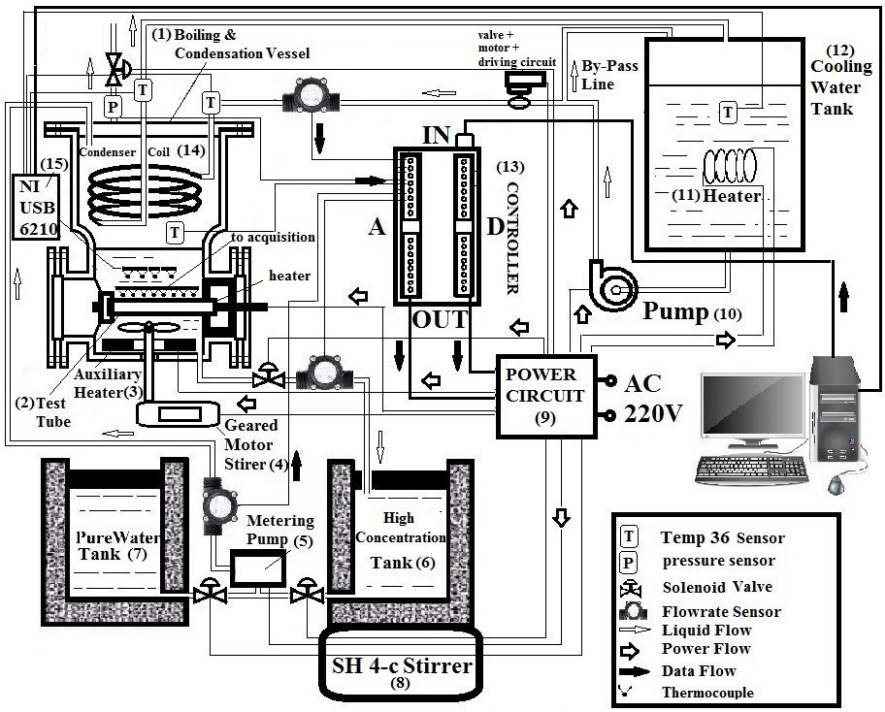

Figure C.1 The Detailed Drawing of The Test Rig

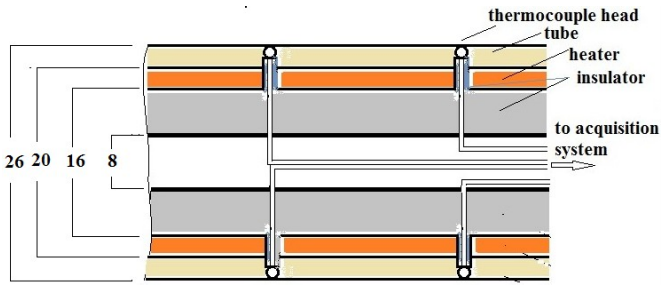

Figure C.2 the test tube, (dimensions are in mm).